Long-Wave Trapping by Oceanic Ridges

RICHARD PAUL SHAW AND WAYNE NEU

Department of Engineering Science, Aerospace Engineering and Nuclear Engineering, F.E.A.S., State University of New York, Buffalo 14214

(Manuscript received 31 March 1981, in final form 13 July 1981)

ABSTRACT

Long waves are affected by bottom topography and under certain conditions may be trapped along topographical contours which then act as wave guides transmitting wave energy for great distances with little loss. This study examines waves trapped along a submerged ridge described by straight parallel bottom contours which in cross section are composed of constant-slope segments bounded on either side by constant-depth segments. Solutions are found for time harmonic waves periodic in the along-ridge direction and of exponential decay behavior normal to the ridge over the constant-depth segments. Over the linearly varying topography describing the ridge, the solution is in terms of two Kummer (or Whittaker) functions. For a given geometry, a dispersion equation is obtained relating the wave frequency to the along-ridge wavenumber for trapped waves. A constant Coriolis parameter is included, but primary interest is on class I (high-frequency) waves. A comparison of cutoff frequencies predicted for this piecewise continuous ridge and those for a segmented constant-depth ridge is made, and the appropriate scaling factors between the two results are discussed. Comparisons of the phase and group velocities are also made for these cases.

1. Introduction

The study of topographically trapped waves appears to have begun with Stokes' (1846) description of edge waves on a linear topography of straight parallel bottom contours. While this solution was originally felt to be of only theoretical interest, observations during the last few decades have given new physical significance to these forms of waves. This study shall examine the influence of one-dimensional (parallel contours) bottom topography on the trapping and guiding of ocean wave energy. In particular, linearized long-wave theory, for a homogeneous perfect fluid, with rotation is used over topographies which consist of constant and linear depth cross-sectional variations. Before further detail on this study, a review of some background material is in order. LeBlond and Mysak (1978) provide an important overview of the area of ocean waves; more specific results are given below. Eckart (1951) showed that, for shallow-water theory, the Stokes solution was just the lowest mode of an infinity of modes and Ursell (1952) obtained these results generalized to three-dimensional linearized water-wave theory leading to a mixed spectrum of discrete and continuous eigenfrequencies. Reid (1958) showed that the earth's rotation would have a modifying effect on these class I or inertio-gravitational waves (which can propagate in both directions along a north-south coast albeit with differing phase speeds for nonzero rotation) and would also allow for a class II or quasi-geostrophic wave which can propagate in only one direction and can not exist in the absence of rotation.

The differences between class I (high-frequency) and class II (low-frequency) shallow-water waves has lead to two roughly distinct classes of literature—those primarily concerned with relatively nearshore phenomena, e.g., tsunami periods and shorter (under 1 h), see Munk *et al.* (1956), and those concerned with oceanographic-scale phenomena, e.g., periods of the order of days. Clearly, these interests overlap but a distinction can be made on the basis of the wave frequency ω versus the Coriolis frequency f. If $\omega \gg f$, it is the edge wave or class I wave which is usually of primary interest while if $\omega \ll f$, it is the quasi-geostrophic or class II wave. This study is directed at the former; the second class of waves will be discussed in a later paper.

It is clear from the various formulations of these problems that waves may be trapped over completely submerged topography, as shown by Hidaka (1976)—see Meyer (1971) for a review of resonance of unbounded water bodies, Shen *et al.* (1968) for a geometrical optics approach and Buchwald (1968) for a solution of the piecewise constant-depth case and a discussion of the general nature of such problems as solutions to Sturm-Liouville equations. One aim of the present study is to see how well the piecewise constant-depth solution represents solutions

0022-3670/81/101334-11$06.75

for gently sloping bottom topographies by comparison to another analytical solution for piecewise linear depths. The solution to this linear topography was noted by Shaw (1974) and Guza and Davis (1974) in terms of Kummer functions, but no numerical results were given until Shaw (1977), due to an apparent lack of tables and/or subroutines for these functions.

While the question of resonances is difficult enough for the trapped-wave problem, the prior question of how energy arrives to be trapped also must be considered. For trapped waves, the energy may be supplied by nonlinear effects, local atmospheric forcing or even local seismic disturbances since a linearized, unforced theory only provides for the persistence of such trapped motions once begun. However, it must be pointed out that total wave trapping is exceptional; Longuet-Higgins (1969) has shown that curved topographies lead to "leaky" trapped modes. Rather than negating the importance of trapped-wave studies, these results enhance them, since this provides a simple mechanism for these cases by which incident wave energy can be fed into the resonating system. Alternatively, for a ridge of finite length, wave energy may enter the system at the ends, exciting a resonance along the ridge as well as across the ridge. This mechanism may be particularly appropriate at locations where a long ridge terminates at a coastline, e.g., the Chatham rise off of the east coast of New Zealand (Heath, 1979).

2. Formulation

The problems considered here are concerned with wave-energy trapping by a topography with either a one-dimensional piecewise discontinuous cross section composed of constant-depth segments or a piecewise continuous cross section composed of linear-depth segments. Although rotation of an f plane will be included, emphasis will be on first class surface gravity waves on a homogeneous fluid where Coriolis effects are a modifying rather than a fundamental influence.

The vertically integrated equations of motion in a coordinate system with contours parallel to the y axis are

$$\partial u/\partial t - fv = -g\partial\zeta/\partial x, \quad (1a)$$

$$\partial v/\partial t + fu = -g\partial\zeta/\partial y, \quad (1b)$$

$$\partial(Hu)/\partial x + \partial(Hv)/\partial y = -\partial\zeta/\partial t, \quad (1c)$$

with water depth H and Coriolis parameter f.

Assuming time harmonic behavior $\exp(-i\omega t)$ and periodic along-contour behavior $\exp(iky)$ allows these equations to be solved separately for the horizontal velocities u, v and free-surface elevation ζ.

$$u = (-i\omega g\partial\zeta/\partial x + ifkg\zeta)/(\omega^2 - f^2), \quad (2a)$$

$$v = (\omega gk\zeta - fg\partial\zeta/\partial x)/(\omega^2 - f^2), \quad (2b)$$

$$H(x)\frac{d^2\zeta}{dx^2} + \frac{dH(x)}{dx}\frac{d\zeta}{dx} + \left[\frac{\omega^2 - f^2}{g} - \frac{fk}{\omega}\frac{dH}{dx} - Hk^2\right]\zeta = 0. \quad (2c)$$

These equations may be nondimensionalized with respect to some reference depth H_R and length L, i.e., using

$$\left.\begin{aligned} \bar{\zeta} &= \zeta/H_R, \quad \bar{h} = H/H_R \\ (\bar{x}, \bar{y}) &= (x, y)/L, \quad \bar{k} = kL \\ (\bar{u}, \bar{v}) &= (u, v)(\omega L/gH_R) \\ \bar{f} &= f/\omega, \quad \bar{\omega} = \omega L/(gH_R)^{1/2} \end{aligned}\right\}. \quad (3)$$

Eqs. (2) become

$$\bar{u} = i(\bar{f}\bar{k}\bar{\zeta} - \partial\bar{\zeta}/\partial\bar{x})/(1 - \bar{f}^2),$$

$$\bar{v} = (\bar{k}\bar{\zeta} - \bar{f}\partial\bar{\zeta}/\partial\bar{x})/(1 - \bar{f}^2),$$

$$\bar{h}(\bar{x})\frac{d^2\bar{\zeta}}{d\bar{x}^2} + \frac{d\bar{h}(\bar{x})}{d\bar{x}}\frac{d\bar{\zeta}}{d\bar{x}} + \left[\bar{\omega}^2(1 - \bar{f}^2) - \bar{k}\bar{f}\frac{d\bar{h}}{d\bar{x}} - \bar{h}\bar{k}^2\right]\bar{\zeta} = 0, \quad (4)$$

which will have different solutions for different topographies $\bar{h}(\bar{x})$. The simplest case arises for constant depth, for example, H_0 (not necessarily the reference depth) such that $\bar{h}_0 = H_0/H_R$,

$$\bar{h}_0\frac{d^2\bar{\zeta}}{d\bar{x}^2} + [\bar{\omega}^2(1 - \bar{f}^2) - \bar{h}_0\bar{k}^2]\bar{\zeta} = 0, \quad (5)$$

leading to

$$\bar{\zeta} = c_1\exp(+\lambda\bar{x}) + c_2\exp(-\lambda\bar{x}), \quad (6)$$

where λ is defined by the indicial equation $\lambda^2 = \bar{k}^2 - \bar{\omega}^2(1 - \bar{f}^2)/\bar{h}_0$. For values of $\bar{h}_0$ and $\bar{f}$ such that $\bar{k}^2 > \bar{\omega}^2(1 - \bar{f}^2)/\bar{h}_0$, λ is real and the solution for $\bar{\zeta}$ is exponential in $\bar{x}$ while for $\bar{k}^2 < \bar{\omega}^2(1 - \bar{f}^2)/\bar{h}_0$, λ is imaginary and the solution is sinusoidal in $\bar{x}$.

If a linear depth is considered, $\bar{h}(\bar{x}) = [\delta + \gamma\bar{x}]$, this equation reduces to

$$(\delta + \gamma\bar{x})\frac{d^2\bar{\zeta}}{d\bar{x}^2} + \gamma\frac{d\bar{\zeta}}{d\bar{x}} + [\bar{\omega}^2(1 - \bar{f}^2) - \bar{k}\bar{f}\gamma - (\delta + \gamma\bar{x})\bar{k}^2]\bar{\zeta} = 0. \quad (7)$$

Introduce $z = \delta + \gamma\bar{x}$; this equation is then

$$z\frac{d^2\bar{\zeta}}{dz^2} + \frac{d\bar{\zeta}}{dz} + \left[\frac{\bar{\omega}^2(1 - \bar{f}^2) - \bar{k}\bar{f}\gamma}{\gamma^2} - \frac{\bar{k}^2}{\gamma^2}z\right]\bar{\zeta} = 0, \quad (8)$$

which is reducible to the confluent hypergeometric equation as seen in Erdelyi *et al.* (1953, Chap. 6,

Section 2). Two distinct cases must be considered. If $\bar{k} = 0$ (the wave is traveling parallel to the x axis), Eq. (8) corresponds to (8) of this reference and the solutions are $C_0[2\bar{\omega}(1 - \bar{f}^2)^{1/2}z^{1/2}/\gamma]$, where C_0 represents any two independent solutions to the zero-order Bessel equation. If $\bar{k} \neq 0$, we have the form of Eq. (6) of this reference with solutions $\exp(-\xi/2) \times F(a, c, \xi)$, where

$$a = \frac{(1 - \bar{f})}{2} + \frac{\bar{\omega}^2(1 - \bar{f}^2)}{2\gamma\bar{k}},$$

$$c = 1,$$

$$\xi = -\frac{2\bar{k}z}{\gamma}.$$

F represents any two independent solutions to the confluent hypergeometric equation. Since $c = 1$, one of the solutions will be of logarithmic form.

This form is appropriate for $\xi > 0$. For $\xi < 0$, the Kummer transformation leads to the form $\exp(+\xi/2) \times F(a', 1, -\xi)$, where $a' = 1 - a = (1 + \bar{f})/2 - \bar{\omega}^2(1 - \bar{f}^2)/2\gamma k$.

The solution in regions of nonzero, constant-slope bottom topography, for $\bar{k} \neq 0$, therefore (using the notation of Abramowitz and Stegun, 1964)

$$\begin{aligned}\bar{\zeta} &= \exp(-\xi/2)[c_3M(a, 1, \xi) + c_4U(a, 1, \xi)] \quad \xi > 0,\\ &= \exp(+\xi/2)[c_3M(a', 1, -\xi)\\ &\qquad + c_4U(a', 1, -\xi)] \quad \xi < 0, \quad (9)\end{aligned}$$

where c_3 and c_4 are arbitrary constants. M and U represent the two independent Kummer functions. These solutions also may be expressed in terms of Whittaker functions.

3. Step ridge topography—discontinuous, constant-depth cross section

This problem was discussed by Buchwald (1968) and forms a test case against which the later continuous depth case may be examined. Since constant-depth, discontinuous (piecewise continuous) topographies are much simpler to use than any other topography, it is of great practical interest to know, analytically, how well they may represent a gradually varying topography. The basic comparison will be done for the dispersion equation, in particular for the low-frequency cutoff frequencies and the phase and group velocities.

Consider a cross section defined by three regions of constant depth:

Region I:

$$-\infty < x < -B; \quad H(x) = H_1,$$

Region II:

$$-B < x < +B; \quad H(x) = H_2,$$

Region III:

$$+B < x < +\infty; \quad H(x) = H_3,$$

where coordinates are chosen such that $H_3 \geq H_1$.

Using B and H_1 as reference lengths for horizontal and vertical distances respectively, the solution in region I is

$$\bar{\zeta}_{\mathrm{I}} = A_1 \exp(\lambda_1\bar{x}), \quad (10)$$

where $\lambda_1 = [\bar{k}^2 - \bar{\omega}^2(1 - \bar{f}^2)]^{1/2}$ and the portion of the solution which diverges as $\bar{x} \to -\infty$ is suppressed. In region II, an oscillatory behavior is anticipated, i.e.,

$$\bar{\zeta}_{\mathrm{II}} = A_2 \cos(\lambda_2\bar{x}) + B_2 \sin(\lambda_2\bar{x}), \quad (11)$$

where $\lambda_2 = [\bar{\omega}^2(1 - \bar{f}^2)/\bar{h}_2 - \bar{k}^2]^{1/2}$. Finally, in region III we anticipate another exponentially decaying solution

$$\bar{\zeta}_{\mathrm{III}} = A_3 \exp(-\lambda_3\bar{x}), \quad (12)$$

where $\lambda_3 = [\bar{k}^2 - \bar{\omega}^2(1 - \bar{f}^2)/\bar{h}_3]^{1/2}$.

Clearly, $\bar{k}$ is bounded by $\bar{\omega}[(1 - \bar{f}^2)/\bar{h}_2]^{1/2}$ from above and by $\bar{\omega}(1 - \bar{f}^2)^{1/2}$ from below.

Continuity of surface elevation and mass flow requires

$$\left.\begin{aligned}\bar{\zeta}_{\mathrm{I}}(\bar{x} = -1) &= \bar{\zeta}_{\mathrm{II}}(\bar{x} = -1)\\ \bar{u}_{\mathrm{I}}(\bar{x} = -1) &= \bar{h}_2\bar{u}_{\mathrm{II}}(\bar{x} = -1)\\ \bar{\zeta}_{\mathrm{II}}(\bar{x} = +1) &= \bar{\zeta}_{\mathrm{III}}(\bar{x} = +1)\\ \bar{h}_2\bar{u}_{\mathrm{II}}(\bar{x} = +1) &= \bar{h}_3\bar{u}_{\mathrm{III}}(\bar{x} = +1)\end{aligned}\right\}, \quad (13)$$

leading to a system of four homogeneous linear algebraic equations on $[A_1, A_2, B_2, A_3]$. The determinant of the coefficient matrix of this system must vanish in order to have a nontrivial solution; this defines the dispersion equation. For simplicity, consider the symmetric case $H_1 = H_3$ without rotation $f = 0$. The dispersion equation then reduces to

$$2\bar{h}_2\lambda_1\lambda_2 \cos2\lambda_2 = (\bar{h}_2{}^2\lambda_2{}^2 - \lambda_1{}^2) \sin2\lambda_2. \quad (14)$$

Along the line $\bar{\omega} = \bar{k}$ which forms a lower bound on the allowable values of $\bar{k}$ for trapped waves, $\lambda_1 = 0$ and the dispersion equation reduces to

$$\sin2\lambda_2 = 0, \quad \lambda_2 = n\pi/2; \quad n = 0, 1, 2, 3. \ldots \quad (15)$$

These are the cutoff points, corresponding to

$$\bar{\omega}_n = (n\pi/2)\left|\bar{h}_2/(1 - \bar{h}_2)\right|^{1/2}, \quad (16)$$

$$\bar{k}_n = (n\pi/2)\left|\bar{h}_2/(1 - \bar{h}_2)\right|^{1/2}. \quad (17)$$

The shape of the free surface separates into symmetric and antisymmetric modes. For even n, B_2 is zero and $A_1 = A_3 = \cos(n\pi/2)A_2$, i.e., these are the symmetric modes, while for odd n, A_2 is zero and $A_1 = -A_3 = -\sin(n\pi/2)A_2$, i.e., the antisymmetric modes.

4. Linear ridge topography—continuous linear cross section

Consider a ridge composed of a piecewise continuous, linear cross section defined by

Region I:

$$-\infty < x < -A; \quad H(x) = H_1,$$

Region II:

$$-A < x < 0; \quad H(x) = H_2 - (H_1 - H_2)x/A,$$

Region III:

$$0 < x < B; \quad H(x) = H_2 + (H_3 - H_2)x/B,$$

Region IV:

$$B < x < \infty; \quad H(x) = H_3$$

as shown in Fig. 1. A suitable reference depth is $H_R = H_1$ and reference length $L = A$.

Then in region I, $\bar{h}_1 = 1$ and

$$\bar{\zeta}_I = A_1 \exp(\lambda_1 \bar{x}) + B_1 \exp(-\lambda_1 \bar{x}), \qquad (18)$$

where $\lambda_1 = [\bar{k}^2 - \bar{\omega}^2(1 - \bar{f}^2)]^{1/2}$. Clearly, B_1 must be set equal to zero and $\bar{k}^2 > \bar{\omega}^2(1 - \bar{f}^2)$ to have an exponentially decaying wave as $\bar{x} \to -\infty$.

Similarly in region IV, $\bar{h} = H_3/H_1 = \bar{h}_3$ and

$$\bar{\zeta}_{IV} = A_4 \exp(-\lambda_4 \bar{x}) + B_4 \exp(+\lambda_4 \bar{x}), \qquad (19)$$

where

$$\lambda_4 = [\bar{k}^2 - \bar{\omega}^2(1 - \bar{f}^2)/\bar{h}_3]^{1/2}.$$

Again, we require a decaying solution as $\bar{x} \to +\infty$, and thus $B_4 = 0$ and $\bar{k}^2 > \bar{\omega}^2(1 - \bar{f}^2)/\bar{h}_3$.

Next, in region II, $\bar{h}(x) = \bar{h}_2 - (1 - \bar{h}_2)\bar{x}$ such that $\delta = \bar{h}_2 < 1$ and $\gamma = -(1 - \bar{h}_2) < 0$. Then

$$\bar{\zeta}_{II} = \exp(-\xi_2/2)[A_2 M(a_2, 1, +\xi_2) + B_2 U(a_2, 1, +\xi_2)] \qquad (20)$$

with $\xi_2 = +2\bar{k}[(\bar{h}_2/(1 - \bar{h}_2)) - \bar{x}]$ and $a_2 = \frac{1}{2} - \bar{f}/2 - \bar{\omega}^2(1 - \bar{f}^2)/2(1 - \bar{h}_2)\bar{k}$.

Finally, in region III, $\bar{h}(\bar{x}) = \bar{h}_2 + (\bar{h}_3 - \bar{h}_2)(A/B)\bar{x}$ such that $\delta = \bar{h}_2 < 1$ and $\gamma = (\bar{h}_3 - \bar{h}_2)(A/B) > 0$. Then

$$\bar{\zeta}_m = \exp(+\xi_3/2)[A_3 M(a_3', 1, -\xi_3) + B_3 U(a_3', 1, -\xi_3)], \qquad (21)$$

with $\xi_3 = -2\bar{k}[\bar{h}_2\bar{b}/(\bar{h}_3 - \bar{h}_2) + \bar{x}]$ and $a_3' = (1 + \bar{f})/2 - \bar{\omega}^2(1 - \bar{f}^2)\bar{b}/2\bar{k}(\bar{h}_3 - \bar{h}_2)$. Continuity of free-surface height and mass flux at $\bar{x} = -1$, $\bar{x} = B/A = \bar{b}$ requires

$$\left.\begin{aligned} \bar{\zeta}_I(-1) &= \bar{\zeta}_{II}(-1), & \bar{u}_{II}(0) &= \bar{u}_{III}(0) \\ \bar{u}_I(-1) &= \bar{u}_{II}(-1), & \bar{\zeta}_{III}(\bar{b}) &= \bar{\zeta}_{IV}(\bar{b}) \\ \bar{\zeta}_{II}(0) &= \bar{\zeta}_{III}(0), & \bar{u}_{III}(\bar{b}) &= \bar{u}_{IV}(\bar{b}) \end{aligned}\right\} \qquad (22)$$

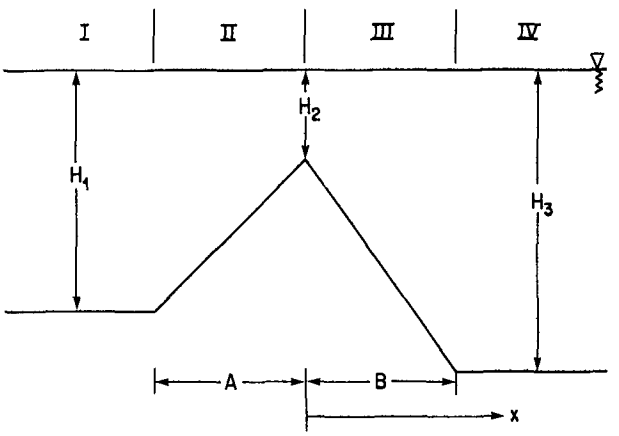

FIG. 1. Linear segment ridge approximation.

or

$$[C_{ij}] \begin{bmatrix} A_1 \\ A_2 \\ B_2 \\ A_3 \\ B_3 \\ A_4 \end{bmatrix} = 0. \qquad (23)$$

Using $\mu_1 = \bar{k}/1 - \bar{h}_2$, $\mu_2 = \bar{h}_2\mu_1$, $\mu_3 = \bar{k}\bar{h}_2\bar{b}/\bar{h}_3 - \bar{h}_2$, $\mu_4 = \bar{k}\bar{h}_3\bar{b}/\bar{h}_3 - \bar{h}_2$ and $\alpha_1 \equiv (a_2, 1, 2\mu_1)$; $\alpha_2 \equiv (a_2, 1, 2\mu_2)$; $\beta_1 \equiv (a_3', 1, 2\mu_3)$; $\beta_2 \equiv (a_3', 1, 2\mu_4)$ and $M' \equiv \partial M(a, 1, \xi)/\partial\xi$, $U' \equiv \partial U(a, 1, \xi)/\partial\xi$, the non-zero values of C_{ij} are

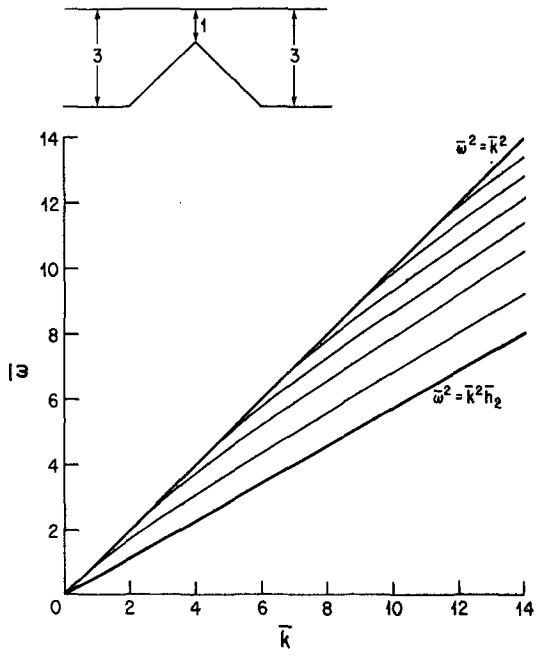

FIG. 2. Symmetric ridge—dispersion equation $H_1 = H_3 = 3$ km, $H_2 = 1$ km, $A = B = 60$ km.

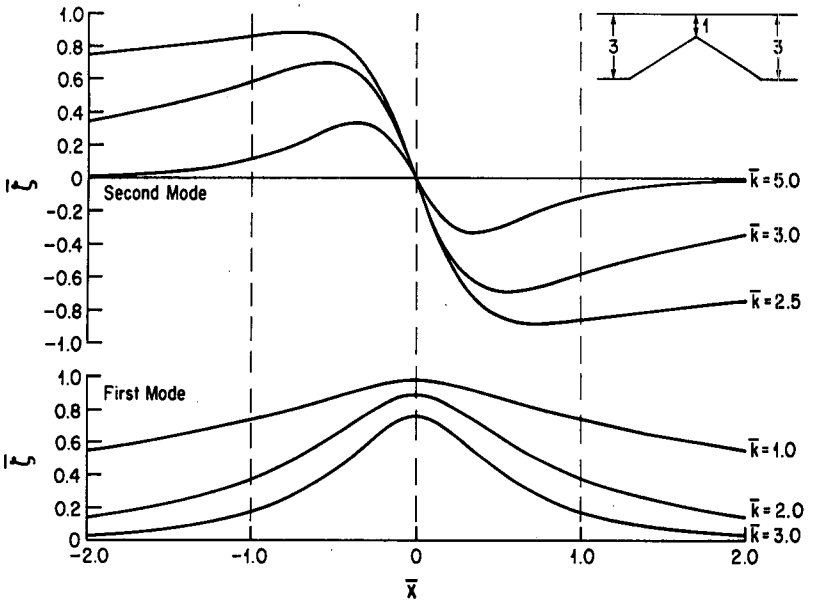

FIG. 3. Symmetric ridge—first and second modes for various values of $\bar{k}$.

$$C_{11} = -\exp(-\lambda_1)$$
$$C_{12} = \exp(-\mu_1)M(\alpha_1)$$
$$C_{13} = \exp(-\mu_1)U(\alpha_1)$$
$$C_{21} = -\lambda_1 \exp(-\lambda_1)$$
$$C_{22} = \bar{k} \exp(-\mu_1)[M(\alpha_1) - 2M'(\alpha_1)]$$
$$C_{23} = \bar{k} \exp(-\mu_1)[U(\alpha_1) - 2U'(\alpha_1)]$$
$$C_{32} = \exp(-\mu_2)M(\alpha_2)$$
$$C_{33} = \exp(-\mu_2)U(\alpha_2)$$
$$C_{34} = -\exp(-\mu_3)M(\beta_1)$$
$$C_{35} = -\exp(-\mu_3)U(\beta_1)$$
$$C_{42} = \bar{k} \exp(-\mu_2)[M(\alpha_2) - 2M'(\alpha_2)]$$
$$C_{43} = \bar{k} \exp(-\mu_2)[U(\alpha_2) - 2U'(\alpha_2)]$$
$$C_{44} = \bar{k} \exp(-\mu_3)[M(\beta_1) - 2M'(\beta_1)]$$
$$C_{45} = \bar{k} \exp(-\mu_3)[U(\beta_1) - 2U'(\beta_1)]$$
$$C_{54} = \exp(-\mu_4)M(\beta_2)$$
$$C_{55} = \exp(-\mu_4)U(\beta_2)$$
$$C_{56} = -\exp(-\lambda_4\bar{b})$$
$$C_{64} = \bar{k} \exp(-\mu_4)[M(\beta_2) - 2M'(\beta_2)]$$
$$C_{65} = \bar{k} \exp(-\mu_4)[U(\beta_2) - 2U'(\beta_2)]$$
$$C_{66} = -\lambda_4 \exp(-\lambda_4\bar{b}).$$

The dispersion equation is then $\det[C_{ij}] = 0$. With some manipulation, this determinant reduces to

$$\begin{vmatrix} M(\alpha_2) - 2M'(\alpha_2) & U(\alpha_2) - 2U'(\alpha_2) \\ \nu_1 M(\alpha_1) - 2M'(\alpha_1) & \nu_1 U(\alpha_1) - 2U'(\alpha_1) \end{vmatrix} \begin{vmatrix} M(\beta_1) & U(\beta_1) \\ \nu_4 M(\beta_2) - 2M'(\beta_2) & \nu_4 U(\beta_2) - 2U'(\beta_2) \end{vmatrix}$$
$$+ \begin{vmatrix} M(\beta_1) - 2M'(\beta_1) & U(\beta_1) - 2U'(\beta_1) \\ \nu_4 M(\beta_2) - 2M'(\beta_2) & \nu_4 U(\beta_2) - 2U'(\beta_2) \end{vmatrix} \begin{vmatrix} M(\alpha_2) & U(\alpha_2) \\ \nu_1 M(\alpha_1) - 2M'(\alpha_1) & \nu_1 U(\alpha_1) - 2U'(\alpha_1) \end{vmatrix} = 0, \quad (24)$$

where $\nu_1 = 1 - \lambda_1/\bar{k}$ and $\nu_4 = 1 - \lambda_4/\bar{k}$.

Again, it is instructive to examine the case of no rotation, $f = 0$, and a symmetric topography, $A = B$ and $H_1 = H_3$. The nondimensionalized problem is then described by the single parameter $\bar{h}_2$. For this case, $\alpha_2 = \beta_1 = \alpha$, $\alpha_1 = \beta_2 = \beta$, and $\nu_1 = \nu_4 = \nu$. The dispersion equation reduces to the product

$$\begin{vmatrix} M(\alpha) - 2M'(\alpha) & U(\alpha) - 2U'(\alpha) \\ \nu M(\beta) - 2M'(\beta) & \nu U(\beta) - 2U'(\beta) \end{vmatrix}$$
$$\times \begin{vmatrix} M(\alpha) & U(\alpha) \\ \nu M(\beta) - 2M'(\beta) & \nu U(\beta) - 2U'(\beta) \end{vmatrix} = 0, \quad (25)$$

which corresponds to symmetric modes ($d\bar{\zeta}/d\bar{x} = 0$ at $\bar{x} = 0$) and antisymmetric modes ($\bar{\zeta} = 0$ at $\bar{x} = 0$), respectively. The cutoff points along the boundary line $\bar{\omega} = \bar{k}$ again may be found using $\lambda_1 = \lambda_4 = 0$ ($\nu = 1$) in Eq. (25).

Numerical results are shown in Figs. 2–5 for the

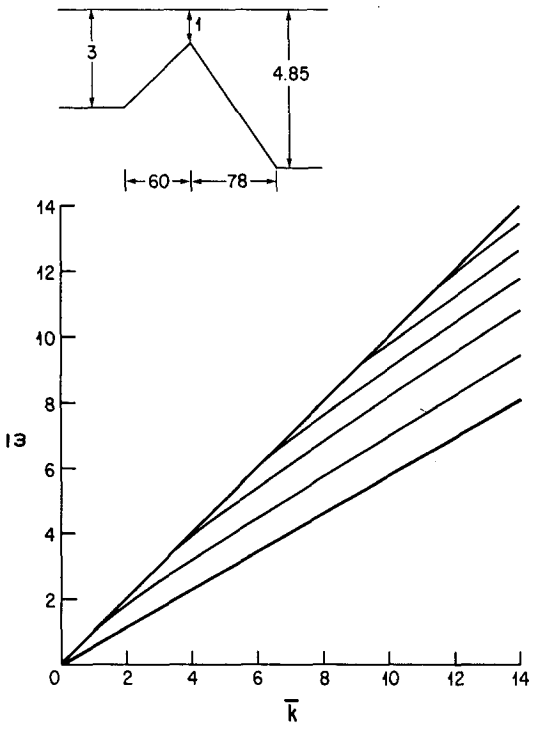

FIG. 4. Asymmetric ridge—dispersion equation $H_1 = 3$ km, $H_2 = 1$ km, $H_3 = 4.85$ km, $A = 60$ km and $B = 78$ km.

symmetric case $H_1 = 3$ km, $H_2 = 1$ km, $H_3 = 3$ km and $A = B = 60$ km and a slightly asymmetric case, $H_1 = 3$ km, $H_2 = 1$ km, $H_3 = 4.85$ km and $A = 60$ km, $B = 78$ km, both without rotation, $f = 0$. Fig. 2 shows the symmetric case dispersion equation followed by Fig. 3 which shows the first two mode shapes. Note that both symmetric and antisymmetric modes result. Fig. 4 shows the asymmetric case dispersion equation followed by Fig. 5 which shows the first two mode shapes; note the slight shift in mode shape caused by the asymmetry.

TABLE 1. Linear ridge cutoff frequencies $\bar{\omega}_n(\bar{h}_2)$.

$\bar{h}_2$ \ n	1	2	3	4	5	6
0.1	1.395	3.220	4.570	6.189	7.595	9.166
0.2	1.791	3.796	5.502	7.360	9.094	10.920
0.3	2.171	4.394	6.424	8.541	10.583	12.678
0.4	2.580	5.064	7.438	9.849	12.223	14.620
0.5	3.053	5.862	8.635	11.400	14.160	
0.6	3.645	6.881	10.150	13.368		
0.7	4.456	8.297	12.249			
0.8	5.800	10.567				

5. Comparison of cutoff frequencies

The cutoff frequencies for a discontinuous, segmented constant depth ridge defined by depth H_1 for $x < -B_C$, H_2 for $-B_C < x < B_C$ and H_3 for $x > +B_C$ are given by

$$\bar{\omega}_n = (n\pi/2)[\bar{h}_2/(1 - \bar{h}_2)]^{1/2},$$

where the depth H_1 and half ridge width B_C are again used as reference lengths, e.g., Buchwald (1968), Shaw and Neu (1979). Corresponding cutoff frequencies may be found for the linear ridge for various values of $\bar{h}_2$; these are shown in Table 1.

The ratio of these cutoff frequencies to those for the constant-depth case varies with $\bar{h}_2$ and slightly with n and is shown in Fig. 6. Here $\bar{\omega}_n$ (constant depth)/$\bar{\omega}_n$ (linear depth) is shown as a function of $\bar{h}_2$ with a range indicated at each $\bar{h}_2$ representing

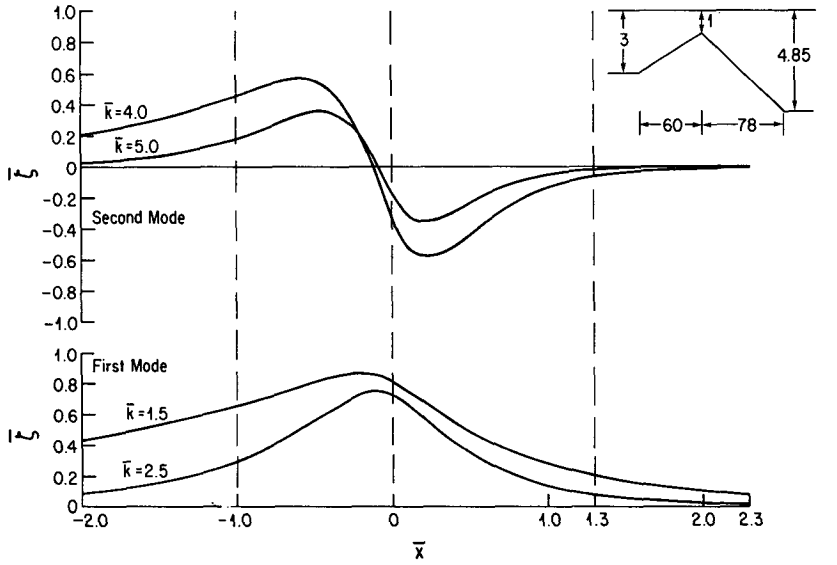

FIG. 5. Asymmetric ridge—first and second modes for various values of $\bar{k}$.

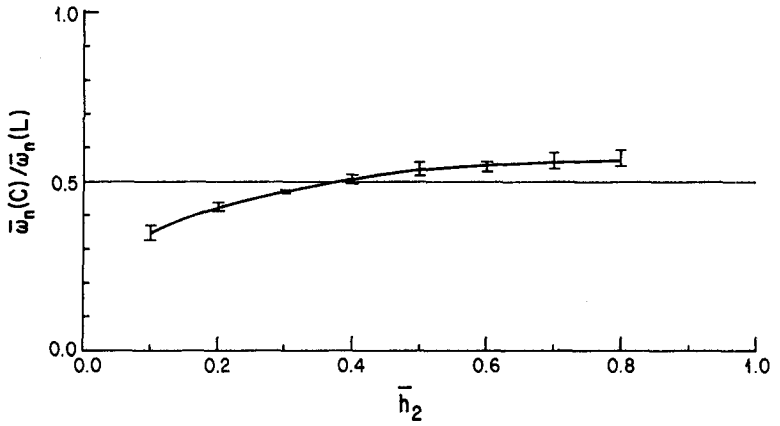

FIG. 6. Ratio of constant depth ridge cutoff frequencies to linear ridge cutoff frequencies as a function of depth ratio $\bar{h}_2$.

the variation with n. For a wide range of values of $\bar{h}_2$, the ratio is ~0.5. This implies that a linear ridge of total width $2B_L$ and a constant depth segment ridge of one-half of this width, $B_C = 0.5\,B_L$, would lead to approximately the same cutoff frequencies. This corresponds to maintaining the same total cross-sectional area of the ridge and is physically appealing as a useful approximation. Of course, this example does not include rotation and is only for the symmetric ridge.

6. Comparison of phase and group velocities

Again, consider symmetric ridges without rotation and define non-dimensional phase and group velocities as $\bar{c} = \bar{\omega}/\bar{k}$ and $\bar{c}_g = d\bar{\omega}/d\bar{k}$ respectively ($\bar{c} = \bar{c}_g = 1$ and $\bar{c} = \bar{c}_g = \bar{h}_2^{1/2}$ corresponds to dimensional velocities of $[gH_1]^{1/2}$ and $[gH_2]^{1/2}$). The group velocity is found by differentiating the appropriate dispersion equation with respect to $\bar{k}$ and then solving for $d\bar{\omega}/d\bar{k}$.

The step ridge topography yields an identical form of the group velocity for both the symmetric and antisymmetric modes. It is given by

$$\frac{d\bar{\omega}}{d\bar{k}} = \frac{\bar{k}}{\bar{\omega}}\left(\frac{\eta + \bar{h}_2\phi}{\eta + \phi}\right), \tag{26}$$

where

$$\eta = \lambda_2{}^2\bar{h}_2{}^2,$$

$$\phi = \lambda_1{}^3 + \lambda_1{}^2\bar{h}_2 + \lambda_1\eta.$$

The behavior of the phase and group velocities

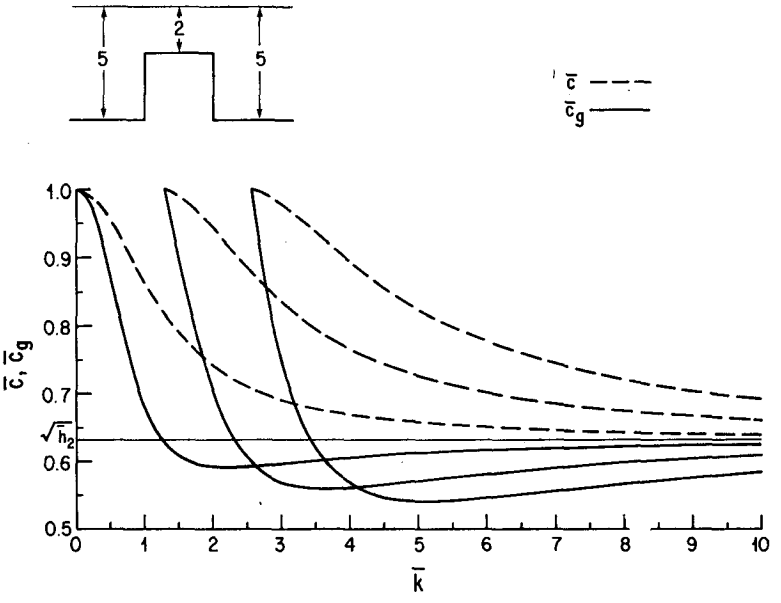

FIG. 7. Phase and group velocities—constant depth ridge $\bar{h}_2 = 0.4$.

in the step ridge case is well documented (e.g., Buchwald, 1968; LeBlond and Mysak 1978), and is shown in Fig. 7 for $\bar{h}_2 = 0.4$. At the cutoff points, $\bar{c} = \bar{c}_g = 1$ and as $\bar{k} \to \infty$, both approach $\bar{h}_2^{1/2}$ asymptotically. However $\bar{c} \to \bar{h}_2^{1/2}$ from above and $\bar{c}_g \to \bar{h}_2^{1/2}$ from below. This implies that there exists a minimum of $\bar{c}_g$ for each mode. Waves of lengths corresponding to this minimum group velocity would encounter less dispersion and therefore are more likely to be observed over oceanic ridges of sufficient length. However, LeBlond and Mysak note that no evidence of these waves has been found despite an attempt by R. A. DeSzoeke (personal communication) to observe them over the Norfolk Island ridge.

Now consider the linear ridge. Define $M^*(a, 1, \xi) = \partial M(a, 1, \xi)/\partial a$ and $U^*(a, 1, \xi) = \partial U(a, 1, \xi)/\partial a$. Upon differentiating the dispersion equation, the antisymmetric modes yield

$$\frac{2\bar{h}_2}{1-\bar{h}_2}\{M'(\alpha)[\nu U(\beta) - 2U'(\beta)] - U'(\alpha)[\nu M(\beta) - 2M'(\beta)]\}$$
$$+ \frac{2}{1-\bar{h}_2}\{M(\alpha)[\nu U'(\beta) - 2U''(\beta)] - U(\alpha)[\nu M(\beta) - 2M''(\beta)]\}$$
$$- \frac{\bar{c}^2}{\bar{k}(1-\nu)}[M(\alpha)U(\beta) - U(\alpha)M(\beta)] + \frac{\bar{c}}{2(1-\bar{h}_2)}[\nu D_1 - 2D_2]$$
$$= \frac{d\bar{\omega}}{d\bar{k}}\left\{\frac{\bar{c}}{1-\bar{h}_2}[\nu D_1 - 2D_2] - \frac{\bar{c}}{\bar{k}(1-\nu)}[M(\alpha)U(\beta) - U(\alpha)M(\beta)]\right\}, \quad (27)$$

where

$$D_1 = [M(\alpha)U(\beta) - U(\alpha)M(\beta)]^*,$$

$$D_2 = [M(\alpha)U'(\beta) - U(\alpha)M'(\beta)]^*.$$

For the symmetric modes, the expression is the same except that $M(\alpha)$ is replaced by $M(\alpha) - 2M'(\alpha)$ and $U(\alpha)$ is replaced by $U(\alpha) - 2U'(\alpha)$ at every occurrence of $M(\alpha)$ and $U(\alpha)$. In the evaluation of these expressions, the derivatives with respect to a, D_1 and D_2 were found numerically.

The results are shown in Fig. 8 where, again, $\bar{h}_2 = 0.4$ and the scale of $\bar{k}$ has been doubled from Fig. 7 to account for the one-half relationship mentioned in the previous section. Note that in this case the group velocity curves are monotonic with no minimum. Fig. 9 compares the dispersion curves of the first two modes for the linear and constant depth cases. The lack of an inflection point in the linear ridge curves is evident here. It is concluded that the minimum group velocity is a consequence of the depth discontinuity in the step model and is not

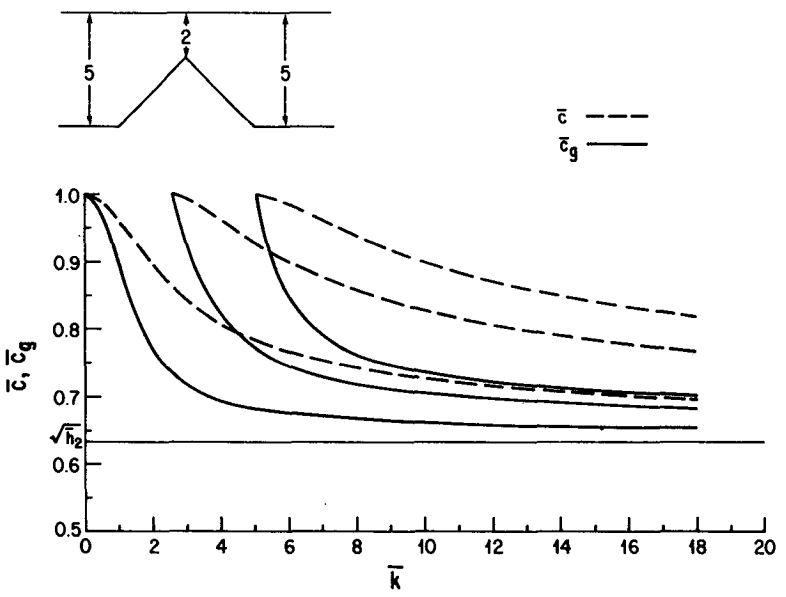

FIG. 8. Phase and group velocities—linear ridge, $\bar{h}_2 = 0.4$.

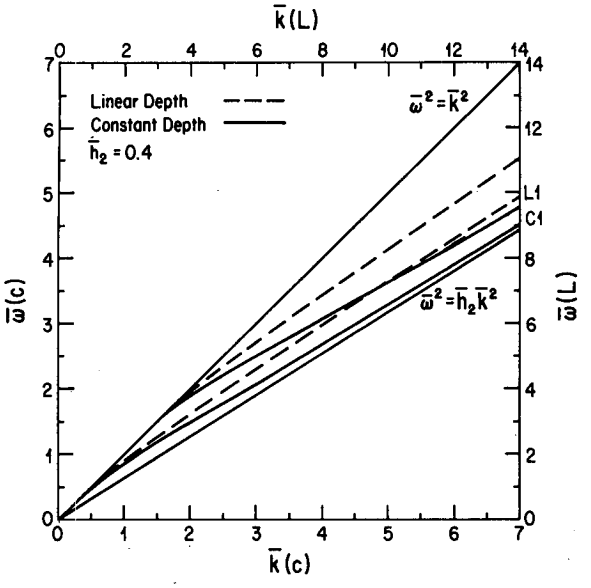

FIG. 9. Comparison of linear and constant depth dispersion equations $\bar{h}_2 = 0.4$.

present in the linear model where the ridge has gently sloping sides.[1]

To further illustrate this point, consider a two step-ridge model, also symmetric and without rotation. The cross section consists of five regions of constant depth:

Region I:

$$-\infty < x < -B; \quad H(x) = H_1$$

Region II:

$$-B < x < -A; \quad H(x) = H_2$$

Region III:

$$-A < x < +A; \quad H(x) = H_3$$

Region IV:

$$+A < x < +B; \quad H(x) = H_2$$

Region V:

$$+B < x < +\infty; \quad H(x) = H_1.$$

Using B and H_1 as horizontal and vertical reference lengths, respectively, the development is analogous to the single step ridge. The solutions in each region are

$$\bar{\zeta}_{\mathrm{I}} = A_1 \exp(\lambda_1 \bar{x}),$$

$$\bar{\zeta}_{\mathrm{II}} = \begin{cases} A_2 \exp(-\lambda_2' \bar{x}) + B_2 \exp(\lambda_2' \bar{x}), & \lambda_2^2 < 0 \\ A_2 \cos\lambda_2 \bar{x} + B_2 \sin\lambda_2 \bar{x}, & \lambda_2^2 > 0 \end{cases}$$

$$\bar{\zeta}_{\mathrm{III}} = A_3 \cos\lambda_3 \bar{x} + B_3 \sin\lambda_3 \bar{x},$$

$$\bar{\zeta}_{\mathrm{IV}} = \begin{cases} A_4 \exp(-\lambda_2' \bar{x}) + B_4 \exp(\lambda_2' \bar{x}), & \lambda_2^2 < 0 \\ A_4 \cos\lambda_2 \bar{x} + B_4 \sin\lambda_4 \bar{x}, & \lambda_2^2 > 0 \end{cases}$$

$$\bar{\zeta}_{\mathrm{V}} = A_5 \exp(-\lambda_1 \bar{x}), \tag{28}$$

where

$$\left.\begin{aligned} \lambda_1 &= (\bar{k}^2 - \bar{\omega}^2)^{1/2}, & \lambda_2' &= (\bar{k}^2 - \bar{\omega}^2/\bar{h}_2)^{1/2} \\ \lambda_2 &= (\bar{\omega}^2/\bar{h}_2 - \bar{k}^2)^{1/2}, & \lambda_3 &= (\bar{\omega}^2/\bar{h}_3 - \bar{k}^2)^{1/2} \end{aligned}\right\}.$$

Note that regions II and IV have solutions which may be either sinusoidal or exponential.

The phase and group velocities of the first four modes for this case are shown in Fig. 10. Although shallow water theory may be invalid for the large values of $\bar{k}$ included in Fig. 10, the mathematical behavior of the solution is of interest. Note, particularly in the third and fourth modes, the existence of two local minimums of the group velocity. Both the phase and group velocities of the third and fourth (and higher) modes begin to approach $\bar{h}_2^{1/2}$ before dropping off to $\bar{h}_3^{1/2}$.

Now return to the forms of the solution over the two step ridge. By examining a branch of the dispersion relation, it is found that at first the solutions in regions II, III and IV are all sinusoidal. As $\bar{\omega}$ and $\bar{k}$ move out along the dispersion curve, λ_2 becomes smaller and reaches zero. Beyond this point, the solutions in regions II and IV become exponential. The wave is then trapped over the top portion of the ridge only.

A similar situation exists in the linear ridge model which may be illustrated through appeal to the approximation of ray theory. Consider a wavefront over the linear ridge whose normal makes an angle θ with the x axis. Denote this angle at the peak ($x = 0$) by θ_0. It is determined by

$$\sin\theta_0 = \frac{\bar{k}\bar{h}_2^{1/2}}{\bar{\omega}}. \tag{29}$$

As the wave moves away from the peak and out over the slope, it begins to turn back toward the peak. Along this arc

$$\sin\theta = \frac{\bar{k}\bar{h}(x)^{1/2}}{\bar{\omega}}. \tag{30}$$

When the wave reaches its turning point, $\theta = 90°$, the nondimensional depth may be denoted by $\bar{h}_T$. From Eq. (30)

$$\bar{h}_T^{1/2} = \frac{\bar{\omega}}{\bar{k}} = \bar{c}. \tag{31}$$

Thus, it is seen that at the cutoff points on the dispersion curve, $\sin\theta_0 = \bar{h}_2^{1/2}$ and $\bar{h}_T^{1/2} = 1$, i.e., the turning point is located over the outer boundary of the ridge. As $\bar{k}$ and $\bar{\omega}$ move out along the dis-

[1] In review, it was mentioned by one of the reviewers that minimum group velocities are found for parabolic and exponential ridge models; these results are expected to be published in the near future.

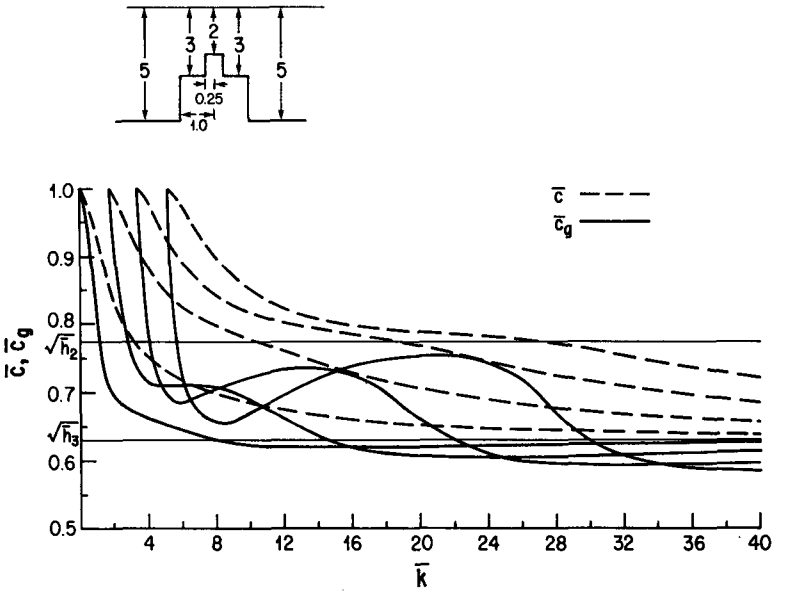

FIG. 10. Phase and group velocities—two-step ridge $H_1 = 5$ km, $H_2 = 3$ km, $H_3 = 1$ km, $A = 0.25\,B$.

persion curve, θ_0 increases and the turning point moves in toward the peak, decreasing the effective width of the ridge. The exponential decay of the free-surface elevation begins at the turning point and extends over the remaining portion of the ridge as well as the bounding constant-depth region on each side. This can be seen in a closer examination of the mode shapes of Figs. 3 and 5. This movement of the turning point and narrowing of the effective width of the linear ridge may account for the increase with $\bar{k}$ of the difference between the linear and step-ridge frequencies and the subsequent lack of a minimum group velocity.

7. Conclusion

The comparison of the linear and constant-depth ridge models has shown that, in general, the two models behave similarly. For an overview of wave trapping by ridges, the constant depth model is useful due to its simplicity. However, if one looks at the details of the dispersion equation, some significant differences between the models are found.

It has been seen that the cutoff frequencies of the linear and constant depth ridges compare favorably provided the width of the constant depth ridge is adjusted such that the areas of the ridge cross sections are equal, at least for the symmetric ridge. It is not known how well this relationship holds for the asymmetric ridge.

It also was seen that the minimum of the group velocity found by Buchwald is a consequence of the constant depth approximation in the step ridge model and is not present in the linear ridge model. It is therefore not surprising that trapped waves at such a predicted minimum group velocity, which should suffer little dispersion, have not been observed.

In the review process, it was mentioned by a reviewer that such minimums do exist for other topographies; it will be interesting to see these results when they are published.

Acknowledgment. This research was supported by the Office of Naval Research, Physical Oceanography, under Contract N00014-79-C-0067.

REFERENCES

Abramowitz, M., and I. A. Stegun, 1964: *Handbook of Mathematical Functions*, NBS App. Math. Series 55, U.S. Dept. of Commerce.

Buchwald, V. T., 1968: Long waves on oceanic ridges. *Proc. Roy. Soc. London*, **A308**, 343–354.

Eckart, C., 1951: Surface waves in water of variable depth. Marine Physical Laboratory of the Scripps Institute of Oceanography, Wave Rep. No. 100, S.I.O. Ref. 51-12, 99 pp. (Unpublished manuscript).

Erdelyi, A., W. Magnus, F. Oberhettinger and F. Tricomi, 1953: *Higher Transcendental Functions*. Vol. 1, Bateman Manuscript Project, McGraw Hill, 391 pp.

Heath, R., 1979: Tsunami Amplification in New Zealand due to trapped waves. *IUGG Tsunami Symposium*, Canberra, Dec. 1979 (to be published in proceedings).

Hidaka, K., 1976: Seiches due to a submarine bank. *Topics in Ocean Engineering III*, C. Bretschneider, Ed., Gulf Publishing Co., 137–140.

LeBlond, P. H., and L. A. Mysak, 1978: *Waves in the Ocean*, Elsevier Oceanography Series, Elsevier, 197–302.

Longuet-Higgins, M. S., 1969: On the trapping of long-period waves round islands. *J. Fluid Mech.*, **37**, 773–784.

Meyer, R. E., 1971: Resonance of unbounded water bodies. *Mathematical Problems in the Geophysical Sciences*, W. H. Reid, Ed., Amer. Math. Soc., 189–228.

Munk, W. H., F. E. Snodgrass and G. Carrier, 1956: Edge waves on the continental shelf. *Science*, **123**, 127–132.

Reid, R. O., 1958: Effect of Coriolis force on edge waves, I. Investigation of normal modes. *J. Mar. Res.*, **16**, 109–144.

Shaw, R. P., 1974: Long waves on linear topographies. JTRE Internal Report No. 119, Haw. Inst. of Geophysics, Honolulu.

——, 1977: Long waves obliquely incident on a continental slope and shelf with a partially reflecting coastline. IUGG Tsunami Symposium, Ensenada, Mexico (also see 1979 Marine Geodesy 2(1): 1–14).

——, and W. Neu, 1979: Long wave trapping by parallel bottom contours. *Proceedings of IUGG Tsunami Symposium*, Canberra, Australia (in press).

Shen, M. C., R. E. Meyer and J. B. Keller, 1968: Spectra of water waves in channels and around islands. *Phys. Fluids*, **11**, 2289–2304.

Stokes, G. G., 1846: Report on recent researches in hydrodynamics. *Rep. 16th Meeting Brit. Assoc. Adv. Sci.*, Southampton, 1846. Murray, London, pp. 1–20. (Also see *Math. Phys. Pap.*, **1**, p. 167.)

Ursell, F., 1952: Edge waves on a sloping beach. *Proc. R. Soc. London*, **A214**, 79–97.